Microstrip Open-Loop Resonator With Multispurious Suppression

Kuo-Sheng Chin, *Member, IEEE*, Yi-Chyun Chiang, *Member, IEEE*, and Jen-Tsai Kuo, *Senior Member, IEEE*

***Abstract*—A compact open-loop resonator with multispurious suppression is proposed. When excited symmetrically, the resonator shows two tunable transmission zeros. By adjusting the open-end gap capacitance, one of the zeros is placed near the passband and the other is tuned to collocate with the leading two degenerated higher order resonances, so that the circuit has a sharp transition as well as a wide upper stopband. The experimental circuit shows the first spurious peak occurs at four times the passband frequency $(4f_o)$, and the measurement shows good agreement with the theoretic prediction.**

***Index Terms*—Bandpass filter (BPF), microstrip circuit, spurious suppression, stepped-impedance resonator (SIR), transmission zero.**

I. Introduction

MINIATURIZATION and wide rejection bandwidth are highly desirable for bandpass filters (BPFs) in radio frequency (RF) front ends of wireless communication systems. BPFs with a single resonator are attractive because they are compact and have a low inband insertion loss. Making planar resonators compact, the open-loop square ring [1], [2] and the hairpin [3] structures can be used. In general, single-resonator BPFs may have poor transition bands since its order is low. In addition, a uniform resonator inherently has spurious passbands at higher order resonances which may seriously degrade BPF performance in the upper stopband.

There have been numerous effective approaches for spurious suppression. The slow-wave resonators [1] and the stepped-impedance resonators (SIRs) [3], [4] push the spurious resonances to higher frequencies so as to extend the upper stopband. A low-pass or bandstop circuit can also be incorporated into a BPF for suppressing the unwanted spurious passbands [5]. By incorporating the ground-plane aperture [6] or the photonic bandgap configuration [7] into the design, the upper stopband can also be extended. The tradeoff, however, includes extra inband insertion loss and increased circuit size.

Manuscript received December 22, 2006; revised May 8, 2007. This work was supported in part by the National Science Council of Taiwan, R.O.C., under Grants NSC 95-2221-E-009-037-MY2 and NSC 95-2221-E-182-012.

K.-S. Chin and Y.-C. Chiang are with the Department of Electronic Engineering, Chang Gung University, Taoyuan 333, Taiwan, R.O.C. (e-mail: kschin@mail.cgu.edu.tw).

J.-T. Kuo is with the Department of Communication Engineering, National Chiao Tung University, Hsinchu 300, Taiwan, R.O.C. (e-mail: jtkuo@mail.nctu.edu.tw).

Color versions of one or more of the figures in this letter are available online at http://ieeexplore.ieee.org.

Digital Object Identifier 10.1109/LMWC.2007.901763

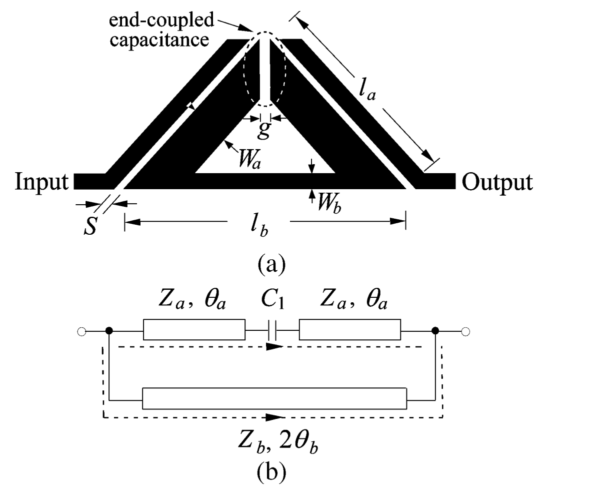

Fig. 1. (a) Triangular open-loop SIR with input/output (I/O) feeders. (b) Equivalent circuit of the resonator.

In this letter, we introduce a novel SIR for filter design with a sharp transition band and multispurious suppression. The SIR is folded as an open triangular loop so that a capacitance exists between its two ends. When the resonator has symmetric input/output, two transmission zeros can be created in upper stopband. The zero placements can be controlled by adjusting the open-end gap capacitance. One of the zeros is placed near the passband so that the BPF has a sharp transition, and the other is tuned to suppress the two leading spurious responses. A BPF is fabricated and measured for demonstration.

II. Triangular Open-Loop SIR

The triangular open-loop resonator shown in Fig. 1(a) is simply a SIR with its two low-impedance sections bent to form an open-end capacitance. Tight coupling is purposely established between the two ends to provide a sufficiently large capacitance and an alternative path for the signal traveling from input to output port. Fig. 1(b) shows the equivalent circuit for analysis. The open-end capacitance C_1 is a part of resonant condition. The dashed lines indicate the two possible signal paths.

Since the resonator is symmetric, the even-odd method [8], [9] can be used for simplifying the analysis. The corresponding resonant frequencies can be derived from the reduced circuits in Fig. 2(a) and Fig. 2(b). By enforcing the input admittance $Y_{\rm in}^o$ to zero, the resonant condition for the odd mode can be derived as

$$Z_a\left(\frac{1}{2\omega C_1}-Z_a\tan\theta_a\right)-Z_b\tan\theta_b\left(Z_a+\frac{\tan\theta_a}{2\omega C_1}\right)=0. \tag{1}$$

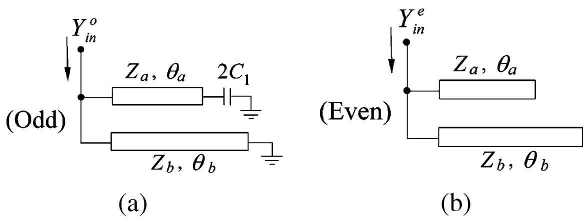

Fig. 2. Reduced equivalent circuit for analysis. (a) Odd mode. (b) Even mode.

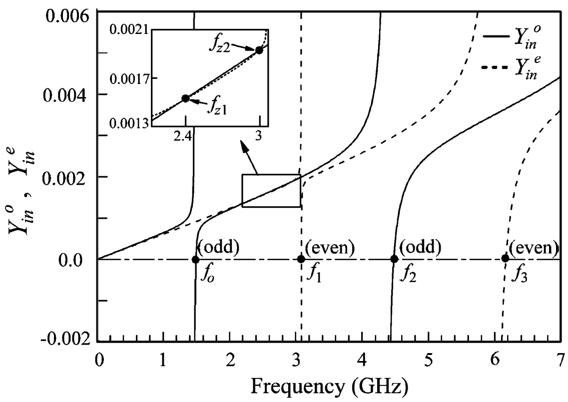

Fig. 3. Calculations of the $Y_{\rm in}^{o}$ and $Y_{\rm in}^{e}$ with $Z_a = Z_b =$ 54.7 $\Omega, l_a = 10$ mm, $l_b = 16$ mm, and $C_1 = 0.05$ pF (a feed-in capacitance of 0.1 pF is assumed).

Similarly, the even mode resonant frequencies can be obtained by letting $Y_{\rm in}^{e} = 0$

$$Z_b \tan\theta_a + Z_a \tan\theta_b = 0. \tag{2}$$

Based on [8], the transmission zeros of the circuit Fig. 1(b) can be calculated by $Y_{\rm in}^{o} = Y_{\rm in}^{e}$

$$Z_b \sin 2\theta_b + Z_a \sin 2\theta_a - \frac{\cos^2\theta_a}{\omega C_1} = 0. \tag{3}$$

Fig. 3 plots $Y_{\rm in}^{o}$ and $Y_{\rm in}^{e}$ versus frequency when $Z_a = Z_b =$ 54.7 Ω, $l_a = 10$ mm, $l_b = 16$ mm, and $C_1 = 0.05$ pF. All resonant frequencies with zero input admittance are marked with dots. It can be seen that the fundamental resonance occurs in the odd mode, and the first higher-order resonance in the even mode, and so forth. As shown in the zoomed window, the intersections of the $Y_{\rm in}^{o}$ and $Y_{\rm in}^{e}$ curves are two transmission zeros, f_{z1} and f_{z2}; both are less than the first spurious f_1. The creation of the two zeros is explained as follows. At f_{z1}, the slant section of the open triangular resonator in Fig. 1(a) is a quarter-wave open stub (including the effect of C_1) so that the feeding point is virtually short-circuited. The zero f_{z2} is resulted from the multipath effect in which C_1 is a portion of one of the two paths for the signal traveling from the input to the output port.

Since both zeros depend on the end-coupled capacitance, Fig. 4 investigates the variations of f_{z1} and f_{z2} versus C_1 up to 0.1 pF. One can observe that $f_{z1} < f_{z2}$ when C_1 >0 and $f_{z1} = f_{z2}$ when C_1 is zero. Also, f_{z1} has a larger variation when C_1 is changed. Thus it can be used for generating a sharp transition band by controlling the value of C_1 to allocate f_{z1} near the passband frequency f_o.

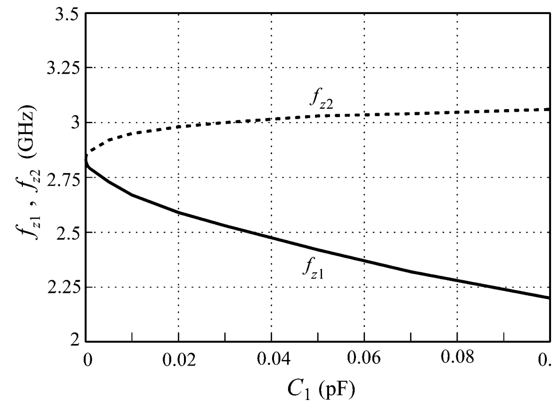

Fig. 4. Transmission zeros versus end-coupled capacitance. $Z_a = Z_b =$ 54.7 $\Omega, l_a = 10$ mm, and $l_b = 16$ mm.

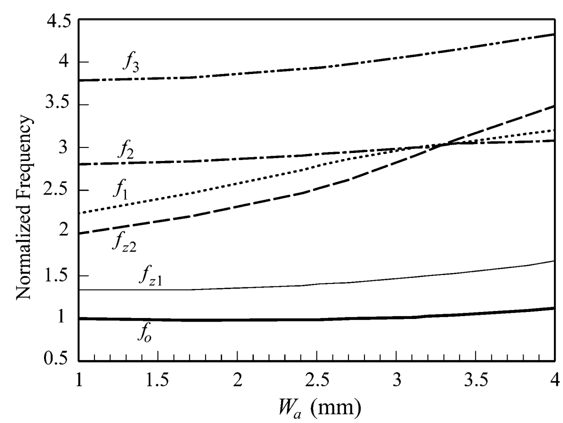

Fig. 5. Changes of normalized resonant frequencies and transmission zeros with respect to W_a for the triangular open-loop BPF. $W_b = 1$ mm, $g = 0.2$ mm, $S = 0.2$ mm, $l_a = 13.58$ mm, $l_b = 19.4$ mm, $\varepsilon_r = 10.2$, and $h = 1.27$ mm.

III. MultiSpurious Suppression

To establish enough coupling between the resonator and the feeders, the line-to-loop coupling structure [10], [11] is adopted. Since one of our objects is to design a BPF with a stopband as wide as possible, the tuning of the resonances and the zeros is of paramount concern. As indicated in (1)–(3), the resonant frequencies and two zeros can be simultaneously tuned by adjusting W_a (or Z_a) since both θ_a and C_1 depend much on it. Fig. 5 plots the zeros and the resonant frequencies for the fundamental mode and the leading three higher order modes against W_a. The software package IE3D is used for circuit simulation. All these frequencies are normalized with respect to the fundamental frequency of a straight half-wave resonator, i.e., $W_a = W_b$. In Fig. 5, when W_a is increased, the two leading even mode frequencies, f_1 and f_3, and the second zero f_{z2} increase faster than the odd mode resonances, f_o and f_2. This can be explained as follows. When W_a is increased, effective electric length θ_a becomes shorter since the leg length l_a is tapered from the outside edge to the inside edge, and this results in a higher resonant frequency. Also, the odd mode currents concentrate at the center base of the triangle, so that the resonant frequencies are just slightly altered by the increase of W_a. On the other hand, the currents of the even mode and the second zero highly concentrate on the legs of the triangle. Consequently, the

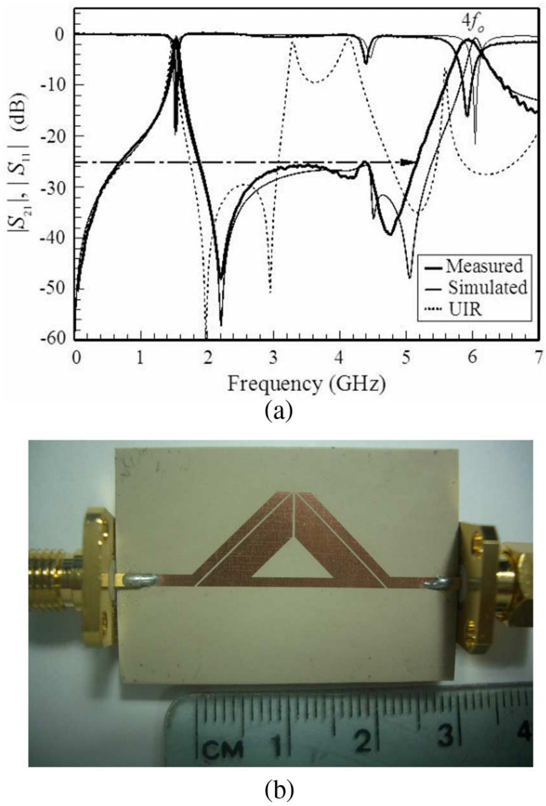

Fig. 6. (a) Simulated and measured responses of the fabricated BPF. (b) Photograph of the fabricated circuit. $f_o = 1.5$ GHz. $W_a = 3.19$, $W_b = 1$, $g = 0.2$, $S = 0.15$, $l_a = 13.58$, and $l_b = 19.4$ (all in mm).

frequencies of f_1, f_3, and f_{z2} increase more rapidly as W_a is increased. As shown in Fig. 5, frequency of f_{z2} is close to those of f_1 and f_2 when $W_a = 3.2$ mm. If f_{z2} can effectively cancel the undesired peaks by f_1 and f_2, the single resonator circuit will have a wide stopband up to $4f_o$. The collocation of the two spurious modes and zero is a general result for the particular open-loop SIR. When W_a is changed, C_1, Z_a and θ_a change at the same time and (1)–(3) can be satisfied at the same frequency simultaneously.

IV. Experimental Results

A single open-loop resonator BPF with $f_o = 1.5$ GHz is designed and fabricated on a substrate with $\varepsilon_r = 10.2$ (RT/duroid 6010) and thickness $h = 1.27$ mm. Fig. 6(a) plots the simulated and measured responses. It can be observed that both responses have good agreement. The rejection level in the upper stopband is better than 25 dB before the spurious passband at $4f_o$. Detailed data show that the inband insertion loss is no larger than 0.5 dB and return loss better than 20 dB. The 3-dB bandwidth is 5%. Note that the first spurious response is at 6 GHz $(4f_o)$. The simulated $|S_{21}|$ response of a triangular open-loop resonator filter with $W_a = W_b$ is also plotted for comparison. Fig. 6(b) shows the photograph of the circuit. The total circuit area is approximately 97.4 mm^2.

V. Conclusion

A single-triangular open-loop resonator for bandpass filter application is presented. The circuit possesses a sharp passband skirt and a wide upper stopband up to four times the passband frequency. The former is achieved by placing a transmission zero near the passband and the latter is by collocating the second zero and the two leading higher order resonances through adjusting the geometric parameter of the resonator. Since only a single resonator is used, the filter has a compact size and exhibits a very good inband insertion loss.

References

[1] J.-S. Hong and M. J. Lancaster, “Theory and experimental of novel microstrip slow-wave open-loop resonator filters,” *IEEE Trans. Microw. Theory Tech.*, vol. 45, no. 12, pp. 2358–2365, Dec. 1997.

[2] D. C. Rebenaque, F. Q. Pereira, J. P. García, A. A. Melcón, and M. Guglielmi, “Two compact configurations for implementing transmission zeros in microstrip filters,” *IEEE Microw. Wireless Compon. Lett.*, vol. 14, no. 10, pp. 475–477, Oct. 2004.

[3] S.-Y. Lee and C.-M. Tsai, “New cross-coupled filter design using improved hairpin resonator,” *IEEE Trans. Microw. Theory Tech.*, vol. 48, no. 12, pp. 2482–2490, Dec. 2000.

[4] J.-T. Kuo and E. Shih, “Microstrip stepped-impedance resonator bandpass filter with an extended optimal rejection bandwidth,” *IEEE Trans. Microw. Theory Tech.*, vol. 51, no. 5, pp. 1554–1559, May 2003.

[5] W.-H. Tu and K. Chang, “Compact microstrip bandstop filter using open stub and spurline,” *IEEE Microw. Wireless Compon. Lett.*, vol. 15, no. 4, pp. 268–270, Apr. 2005.

[6] M. C. Velázquez-Ahumada, J. Martel, and F. Medina, “Parallel coupled microstrip filters with ground-planeaperture for spurious band suppression and enhanced coupling,” *IEEE Trans. Microw. Theory Tech.*, vol. 52, no. 3, pp. 1082–1086, Mar. 2004.

[7] K. F. Chang and K. W. Tam, “Miniaturized cross-coupled filter with second and third spurious responses suppression,” *IEEE Microw. Wireless Compon. Lett.*, vol. 15, no. 2, pp. 122–124, Feb. 2005.

[8] A. C. Kundu and I. Awai, “Control of attenuation pole frequency of a dual-mode microstrip ring resonator bandpass filter,” *IEEE Trans. Microw. Theory Tech.*, vol. 49, no. 6, pp. 1113–1117, Jun. 2001.

[9] C. Lugo and J. Papapolymerou, “Bandpass filter design using a microstrip triangular loop resonator with dual-mode operation,” *IEEE Microw. Wireless Compon. Lett.*, vol. 15, no. 7, pp. 475–477, Jul. 2005.

[10] L.-H. Hsieh and K. Chang, “Dual-mode quasi-elliptic-function bandpass filters using ring resonators with enhanced-coupling tuning stubs,” *IEEE Trans. Microw. Theory Tech.*, vol. 50, no. 5, pp. 1340–1345, May 2002.

[11] R. Wu and S. Amari, “New triangular microstrip loop resonators for bandpass dual-mode filter applications,” in *IEEE MTT-S Int. Dig.*, 2005, pp. 941–944.